

Staying at home is a privilege: evidence from fine-grained mobile phone location data in the U.S. during the COVID-19 pandemic

Xiao Huang^{a*}, Junyu Lu^b, Song Gao^c, Sicheng Wang^{d,e}, Zhewei Liu^f, Hanxue Wei^g

^{a*}Department of Geosciences, University of Arkansas

^bSchool of Community Resources and Development, Arizona State University

^cDepartment of Geography, University of Wisconsin-Madison

^dDepartment of Geography, University of South Carolina

^eEdward J. Bloustein School of Planning and Public Policy, Rutgers University

^fDepartment of Land Surveying and Geo-Informatics, Hong Kong Polytechnic University

^gDepartment of City and Regional Planning, Cornell University

*Email: xh010@uark.edu

This article is to appear in the **Annals of the
American Association of Geographers**

To cite:

Huang, X., Lu, J., Gao, S., Wang, S., Liu, Z., & Wei, H. (2021). Staying at home is a privilege: evidence from fine-grained mobile phone location data in the U.S. during the COVID-19 pandemic. *Annals of the American Association of Geographers*.
doi: 10.1080/24694452.2021.1904819.

Staying at home is a privilege: evidence from fine-grained mobile phone location data in the U.S. during the COVID-19 pandemic

The Coronavirus disease 2019 (COVID-19) has exposed and, to some degree, exacerbated the social inequity in the U.S. This study reveals the correlation between demographic/socioeconomic variables and home-dwelling time records derived from large-scale mobile phone location tracking data at the U.S. Census Block Group (CBG) level in twelve most-populated Metropolitan Statistical Areas (MSAs) and further investigates the contribution of these variables to the disparity in home-dwelling time that reflects the compliance of stay-at-home orders via machine learning approaches. We find statistically significant correlations between the increase in home-dwelling time (∇_{HDT}) and variables that describe economic status in all MSAs, which is further confirmed by the optimized Random Forest models, as median household income and percentage of high income are the top two most important variables in predicting ∇_{HDT} . The partial dependence between median household income and ∇_{HDT} reveals that the contribution of income to ∇_{HDT} is place-dependent, non-linear, and different given varying income intervals. Our study reveals the luxury nature of stay-at-home orders with which lower-income groups may not afford to comply. Such disparity in responses under stay-at-home orders reflects the long-standing social inequity issues in the U.S., potentially causing unequal exposure to the COVID-19 that disproportionately affects the vulnerable populations. We must confront systemic social inequity issues and call for a high-priority assessment of the long-term impact of COVID-19 on geographically and socially disadvantaged groups.

Keywords: COVID-19; mobile phone data; stay-at-home orders; social inequity; Random Forest.

1 Introduction

The Coronavirus disease 2019 (COVID-19) caused by the severe acute respiratory syndrome coronavirus-2 (SARS-CoV-2) has been a global threat that leads to many health, economic, and social challenges. The World Health Organization (WHO) declared COVID-19 as a pandemic on March 11, 2020. Two days after, the U.S. declared the National Emergency (March 13, 2020), stating the severity of the situation and urging local governments and organizations to join forces. At the time of writing, we are still witnessing widespread community transmission of COVID-19. As of October 18, 2020, there had been a total of 40,118,333 infections and 1,114,749 deaths (WHO 2020). The U.S., as one of the global epicenters of the disease, accounts for 20.1% of the global infections (8,065,615 infections) and 19.6% of the global deaths (218,131 deaths) (WHO 2020).

Following the lockdown of the earlier epicenter city of Wuhan in China, social distancing, aiming to restrain the spread, has gradually emerged as one of the most common and effective non-pharmaceutical control measures to reduce person-to-person contact (Wilder-Smith and Freedman 2020). Studies have discovered that the implementation of strong social distancing measures leads to the reduction in mobility and the increase in home-dwelling time, largely responsible for the reduced transmission of SARS-COV-2 in countries that include China (Kraemer et al. 2020), South Korea (Shim et al. 2020), Italy (Remuzzi and Remuzzi 2020), and France (Stoecklin et al. 2020).

In the U.S., the stay-at-home orders (or similar mitigation measures) have been issued by the Federal and local governments to encourage residents to limit their outdoor activities and large gatherings. During the stay-at-home orders, the majority of non-essential businesses were closed to further reduce the risk of viral transmission. Following the first state-wide stay-at-home order issued in California (March 16, 2020), other states started to adopt similar mitigation strategies. On March 24, 2020, more than half of the U.S. population was under stay-at-home orders, and only ten days later (April 4, 2020), 95% of the U.S. population was suggested to stay at home (Baek et al. 2020). However, the effectiveness of the stay-at-home orders greatly relies on public compliance (Gao et al. 2020). Given the voluntary nature of stay-at-home orders in the U.S., there is a collection of evidence that reveals disparate responses from different communities even under the same order (Huang et al. 2020a; Huang et al. 2020b; Chiou and Tucker 2020).

As Dr. Anthony Fauci, the Director of the National Institute of Allergy & Infectious Diseases, White House Coronavirus Task Force, once stated¹:

"When you're in the middle of a crisis like we are now with the coronavirus, it really does...ultimately shine a very bright light on some of the real weaknesses and foibles in our society."

Such disparity in responses reflects the long-standing social inequity issues in the U.S., potentially causing unequal exposure to the COVID-19 that disproportionately affects the socially disadvantaged groups (Bonaccorsi et al. 2020; Dasgupta et al. 2020). Therefore, it is of great importance to understand whether and how communities respond to government decisions and what drives the disparity in responses under those decisions. Such knowledge not only deepens our understanding of social inequity issues exposed by the COVID-19 pandemic but also benefits the decision-making of the Federal government and local authorities in choosing appropriate responses to the COVID-19 pandemic and future epidemics.

For the COVID-19 pandemic, numerous studies have investigated the disparate reactions in response to stay-at-home orders, and many pieces of evidence at various scales have been found, pointing to the societal construct largely determined by demographic and socioeconomic variables. On the country scale, Barnett-Howell and Mobarak (2020) found that social distancing measures are generally less effective in poor countries, as the poorer people are less willing to, or can not afford to, make economic sacrifices. The spatial models constructed by Oyedotun and Moonsammy (2020) revealed a negative relationship between per capita gross domestic product and attributable deaths in South American countries. Similar patterns are confirmed by Huang et al. (2020a), who conducted a similar study at the U.S. county-level using multi-source mobility datasets and found counties with high income tend to reduce their mobility aggressively. Similar patterns were also found at a much finer scale, as a census tract-level study by Chiou and Tucker (2020) revealed that high-income earners generally spent more time at home during the stay-at-home orders (the access to high-speed Internet plays a vital role). Besides the contribution of financial factors, the disparity in response can be explained

¹ <https://www.businessinsider.com/fauci-covid-19-shows-unacceptable-disparities-for-african-americans-2020-4>

by other quantifiable demographic/socioeconomic variables, such as racial/ethnic composition (Czeisler et al. 2020; Huang et al. 2020b), educational attainment (Gray et al. 2020), and commuting modes (Huang et al. 2020a). Other factors that involve risk awareness (Jones 2020; Barrios and Hochberg 2020; Brodeur et al. 2020), belief in science (Briscese et al. 2020), and political affiliations (Painter and Qiu 2020), are also proved to be relevant to the compliance of stay-at-home orders, despite that those factors are difficult to be quantified and accessed.

Fortunately, the increasing availability of mobile phone location tracking derived mobility datasets with fine-grained spatiotemporal resolution has greatly facilitated the rapid monitoring of human mobility in a spatially explicit manner. Through the examination of the stay-at-home compliance in twelve selected Metropolitan Statistical Areas (MSAs), this study contributes to the existing literature by applying data-driven approaches and by taking advantage of the fine-grained home-dwelling records at the U.S. Census Block Group (CBG) level. We aim to reveal the correlation between demographic/socioeconomic variables and home-dwelling time and further statistically investigate the contribution of these variables to the disparity in home-dwelling time that reflects the compliance of stay-at-home orders. The detailed contributions of this work are summarized as follows:

- We use fine-grained home-dwelling records (aggregated at CBG level) collected from millions of mobile devices to assess and cross-compare the compliance of stay-at-home orders in the top twelve most-populated MSAs in the U.S.
- We reveal the correlation between the increase in home-dwelling time during stay-at-home orders and demographic/socioeconomic variables. We further apply an optimized Random Forest algorithm, a popular machine learning method, to statistically investigate the contribution of these variables to the increase in home-dwelling time.
- We present the feature importance of selected demographic/socioeconomic variables and the performance of the designed Random Forest model in predicting the increase in home-dwelling time based on these variables.
- We discuss how the statistically important variables from the Random Forest model reflect the long-standing social inequity issues in the U.S. and what can be suggested for better policy-making during the COVID-19 pandemic and future epidemics.

2 Study Areas and Datasets

2.1 Study Areas

We select twelve most-populated MSAs in the U.S. as our study areas (Figure 1), according to the MSA Population Totals in 2019 (U.S. Census Bureau 2020a). These twelve MSAs include New York-Newark-Jersey City (New York MSA), Los Angeles-Long Beach-Anaheim (Los Angeles MSA), Chicago-Naperville-Elgin (Chicago MSA), Dallas-Fort Worth-Arlington (Dallas MSA), Houston-The Woodlands-Sugar Land (Houston MSA), Washington-Arlington-Alexandria (D.C. MSA), Miami-Fort Lauderdale-Pompano Beach (Miami MSA), Philadelphia-Camden-Wilmington (Philadelphia MSA), Atlanta-Sandy Springs-Alpharetta (Atlanta MSA), Phoenix-Mesa-Chandler (Phoenix MSA), Boston-Cambridge-Newton (Boston MSA), and San Francisco-Oakland-Berkeley (San Francisco MSA).

Established by the U.S. Office of Management and Budget (OMB), a MSA is delineated as a region that consists of at least one urbanized area with a minimum population of 50,000 (U.S. Census Bureau 2020b). The area defined by the MSA generally receives similar mitigation measures during the COVID-19 pandemic and is typically marked by significant social and economic interaction, thus serving as an ideal geographic unit in this study. In addition, the dense population in MSAs ensures sufficient home-dwelling records. The geographical boundaries of these MSAs are the 2019 TIGER/Line Shapefile products issued by the U.S. Census Bureau.

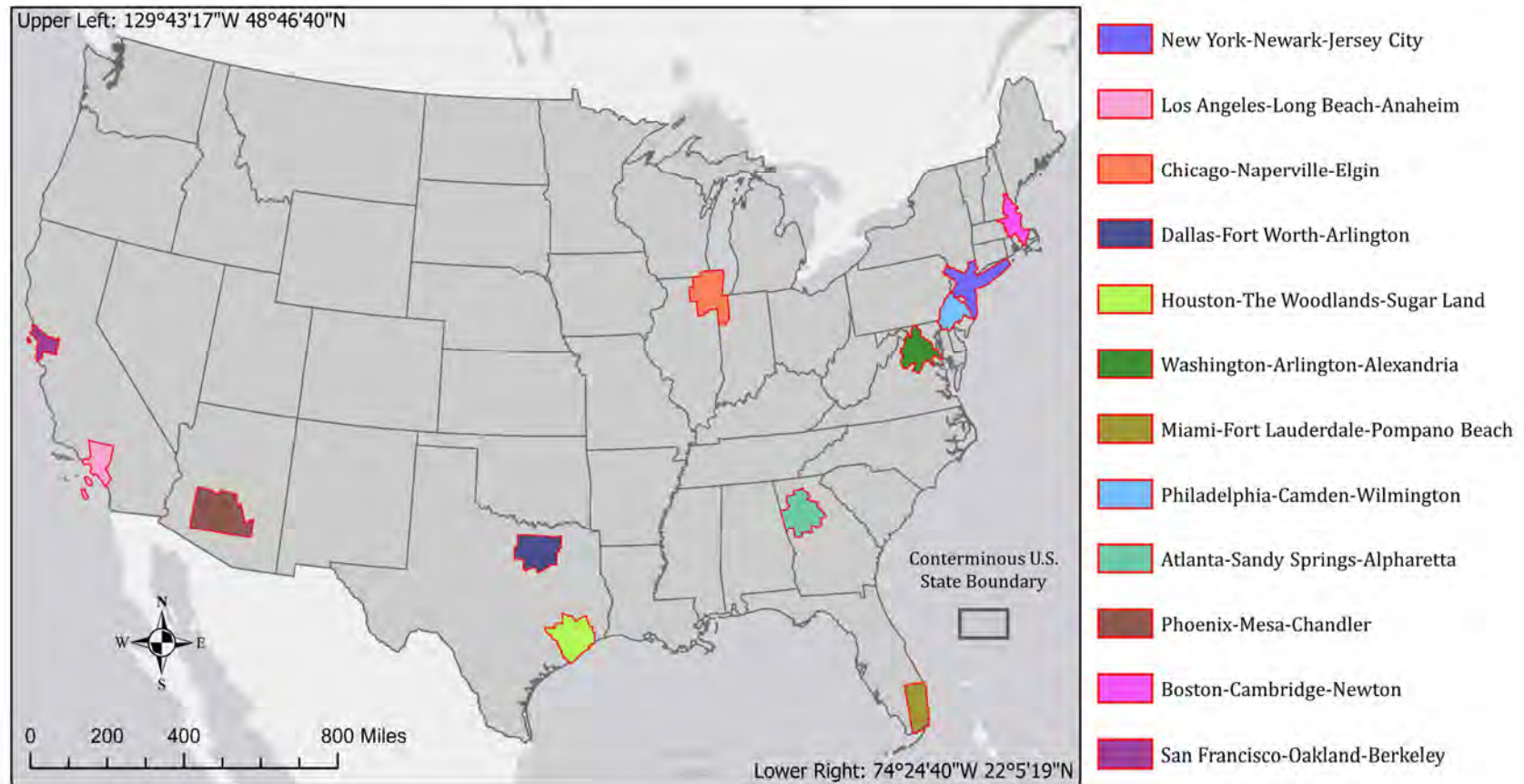


Figure 1. Top twelve most-populated Metropolitan Statistical Areas (MSAs). Basemap credit: Esri, Airbus DS, USGS, NGA, NASA, CGIAR, N Robinson, NCEAS, NLS, OS, NMA, Geodatastyrelsen, Rijkswaterstaat, GSA, Geoland, FEMA, Intermap, and the GIS user community.

2.2 Home-dwelling Time Records

2.2.1 Data Description

The home-dwelling time records are open-sourced by SafeGraph (<https://www.safegraph.com/>), a company that aims to provide insights about physical places by aggregating anonymized location data from numerous applications. The data are collected using a panel of GPS points from around 45 million anonymous mobile devices. Home locations of anonymous device users are first determined based on the common nighttime location of each mobile device over a six-week period to a Geohash-7 granularity ($\sim 153\text{m} \times \sim 153\text{m}$) (SafeGraph 2020). Based on these derived home locations, the home-dwelling time (measured in minutes) for a certain resident is further computed on a daily basis. To enhance privacy, SafeGraph aggregates observed home-dwelling time records to the CBG level by selecting the median value for all available devices within a certain CBG. SafeGraph also excludes CBG information if fewer than five devices visited an establishment in a month from a given CBG to further protect users' privacy. The raw home-dwelling time records cover a total of 219,972 CBGs in the U.S. and span from January 1, 2020, to August 31, 2020 (244 days).

2.2.1 Data Visualization and Data Representativeness

In the study, we select the CBGs that fall within the boundaries of the twelve MSAs. Let HDT_j denote the median value of the home-dwelling time from all available mobile devices in a CBG on day j . Appendix Figure A presents the time-series of daily home-dwelling time in twelve selected MSAs, with the transparency set as 0.01. We further derive the heat map by plotting all the available pairs, i.e., (j, HDT_j) , within the time frame (January 1 to August 31) for each MSA (Figure 2). The impact of COVID-19 on home-dwelling time can be observed, evidenced by the notable increase in home-dwelling time in all MSAs from March to May, 2020. Despite the similarity in the general trend, each MSA presents its unique pattern, revealing the discrepancy in mitigation measures and the inconsistency in responses following these measures. Compared with other MSAs, CBGs in New York MSA (Figure 2h) present high consistency in responses, as a cluster of 1,300 mins in home-dwelling time (out of 1,440 mins in a day) can be observed in March and April. In comparison, CBGs in D.C. MSA (Figure 2l) show rather inconsistent responses, evidenced by the scattered values in the heat map. Besides the

consistency, the intensity of response in selected MSAs also differs. For instance, CBGs in Los Angeles MSA (Figure 2f) show a notably higher increase in home-dwelling time compared with the CBGs in Houston MSA (Figure 2e). Those inconsistencies come from various geographical and socioeconomic factors, which will be our main focus of this study.

To understand the penetration (representativeness) of the home-dwelling time records from SafeGraph, we calculate the median daily device count for each CBG from January 1 to August 31. Following the work by Huang et al. (2020b), the representativeness is defined as the ratio between the median daily device count and the CBG's population (from the American Community Survey 2014-2018 estimates). As shown in Figure 3, the representativeness of one MSA differs from that of another, with Dallas MSA (Figure 3d) showing the highest representativeness while San Francisco MSA (Figure 3k) showing the lowest. Despite the inconsistency among MSAs, the representativeness for most CBGs ranges from 5% - 10%, suggesting a considerably high penetration percentage of the SafeGraph data. In the U.S. panel, SafeGraph's samples correlate highly with the Census population in various demographic and socioeconomic settings (SafeGraph 2019).

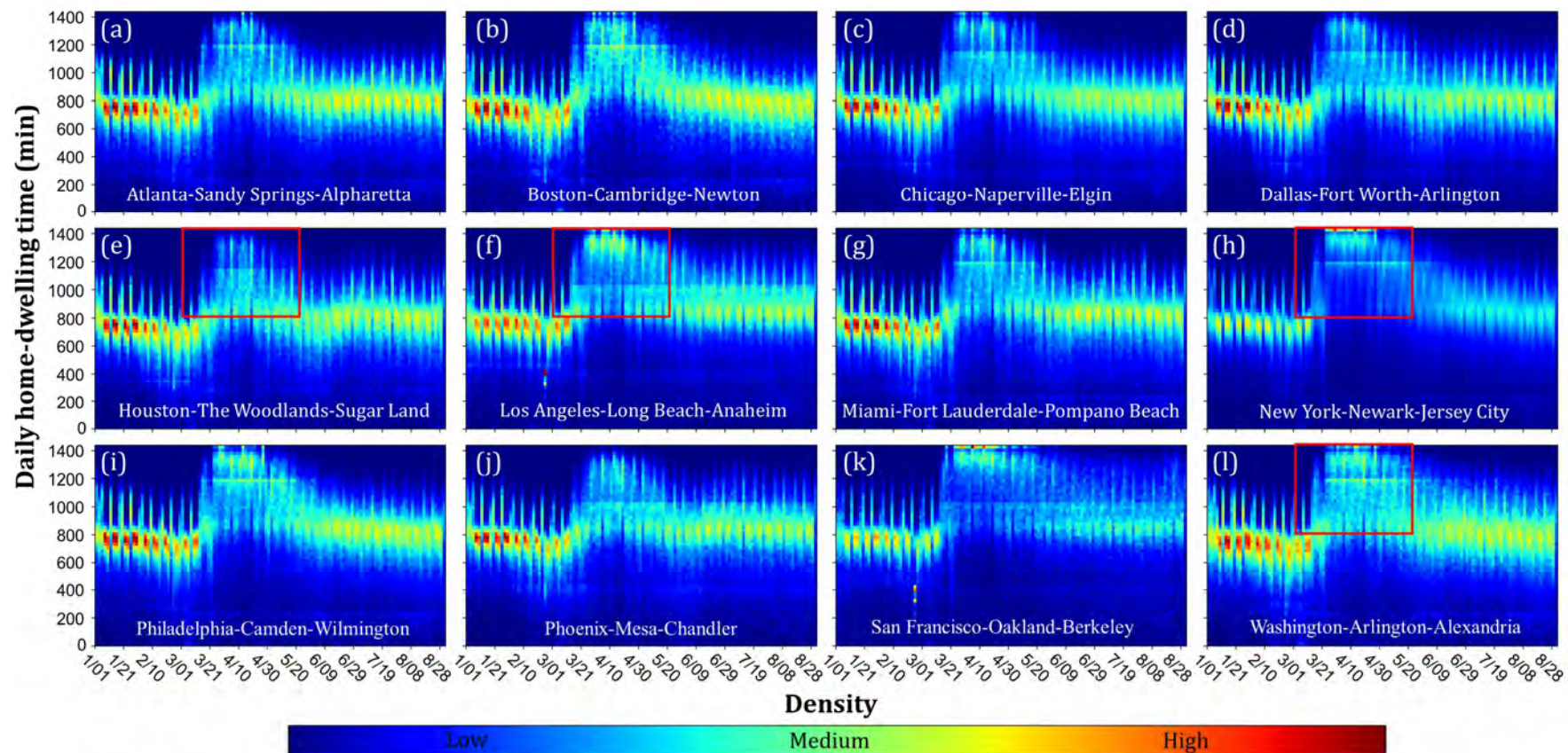


Figure 2. Heat map of daily home-dwelling time for twelve selected MSAs from January 1, 2020, to August 31, 2020. High/low concentrations are marked as red/blue.

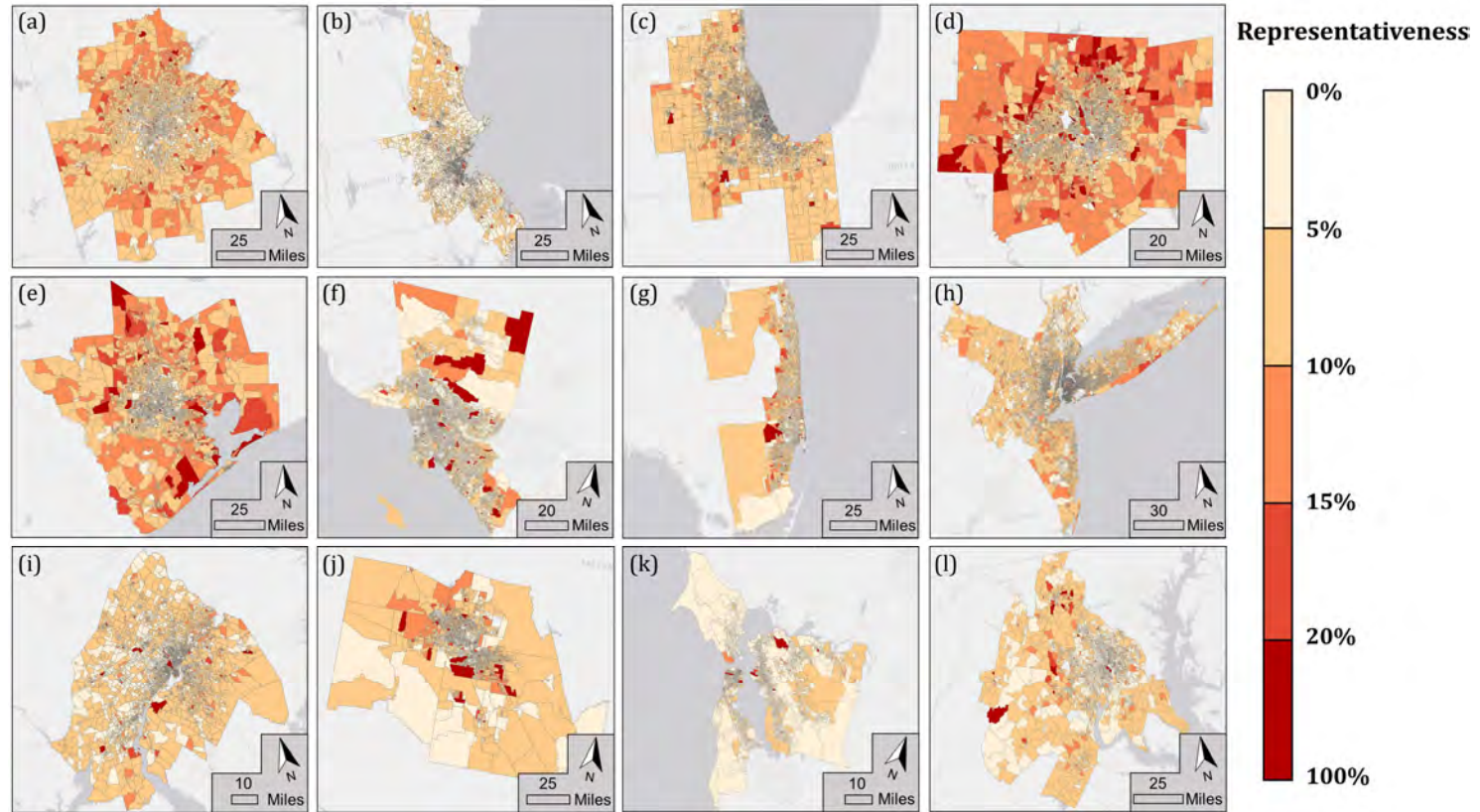


Figure 3. The representativeness of SafeGraph samples in the twelve selected MSAs. (a) Atlanta MSA; (b) Boston MSA; (c) Chicago MSA; (d) Dallas MSA; (e) Houston MSA; (f) Los Angeles MSA; (g) Miami MSA; (h) New York MSA; (i) Philadelphia MSA; (j) Phoenix MSA; (k) San Francisco MSA; (l) D.C. MSA. The CBG boundaries are derived from 2019 TIGER/Line Shapefiles by U.S. Census Bureau (<https://www.census.gov/cgi-bin/geo/shapefiles/index.php>).

2.3 Demographic/Socioeconomic Variables

The demographic and socioeconomic variables in this study are derived from the latest 5-year American Community Survey (ACS) data, i.e., the 2014-2018 ACS 5-year estimates, obtained from Social Explorer (<https://www.socialexplorer.com/>). ACS is an ongoing survey that regularly gathers vital information about population statistics previously contained only in the long form of the U.S Decennial Census. Its 60-month sampling period (from January 1, 2014, to December 31, 2018) increases the statistical reliability when examining small geographical areas, thus believed to be more reliable compared with ACS 1-year and ACS 3-year estimates. Following the design by Huang et al. (2020b), we include and recode twenty-one demographic/socioeconomic variables from five major categories: 1) economic status; 2) race and ethnicity; 3) gender, age, and household type; 4) education; 5) transportation. Numerous studies have proved that these variables are, to some degree, associated with the participation of out-of-home activities (Farner and Páez 2009; Morency et al. 2011; Kuppam and Pendyala 2001). The detailed information regarding the notations and descriptions of these variables is presented in Table 1.

Table 1. Notations and descriptions of the demographic/socioeconomic variables from five major categories.

Variable notations	Descriptions
Economic status	
<i>% low income</i>	Percent of household income less than \$15,000
<i>% high income</i>	Percent of household income greater than \$150,000
<i>median hhinc</i>	Median household income
<i>% unemployment</i>	Unemployment rate
Race and ethnicity	
<i>% white</i>	Percent of White
<i>% black</i>	Percent of Black
<i>% asian</i>	Percent of Asian
<i>% hispanic</i>	Percent of Hispanic
Gender, age, and household type	
<i>% female</i>	Percent of female
<i>% elderly</i>	Percent of age 65 or older
<i>% single parent</i>	Percent of single-parent families among parenting families having children under 18
<i>% child</i>	Percent of age under 5
<i>% schooler</i>	Percent of age 5 to 17
Education	

<i>% low edu</i>	Percent of education equal or less than high school
<i>% grad edu</i>	Percent of education of master, professional, or doctoral degrees
<hr/>	
Transportation	
<i>% work from home</i>	Percent of work from home
<i>% car commuter</i>	Percent of car commuters
<i>% transit commuter</i>	Percent of transit commuters
<i>% short commuter</i>	Percent of commuters with 10 min or shorter trips
<i>% long commuter</i>	Percent of commuters with 40 min or longer trips
<i>% 0car</i>	Percent of 0 car households
<hr/>	

3 Methodology

3.1 Preprocessing

We first select the CBGs that fall within the boundaries of the twelve MSAs, resulting in a total of 59,217 CBGs. SafeGraph applies a panel of GPS points from mobile devices to record residents' daily home-dwelling time. Thus, the number of available devices determines the credibility of the home-dwelling records of a certain CBG. We apply several preprocessing techniques to ensure that the CBGs contain a sufficient number of devices. We calculate the median value of the daily device count for each CBG during the 244-day period and remove CBGs with the median device count lower than 50. The missing value between two consecutive available records is filled via linear interpolation, assuming that home dwell time changes linearly between two consecutive available records. Huang et al. (2020b) reported that the home-dwelling records from SafeGraph contain some CBGs with consecutive zero values, presumably due to the low number of available devices and failure of locating resident's home locations. We further remove CBGs with 0 values that span more than three consecutive days. Table 2 presents the numbers of CBGs in each MSA before and after preprocessing.

Table 2. Numbers of CBGs in each MSA before and after preprocessing.

MSA	Number of CBGs	
	Before preprocessing	After preprocessing
Atlanta	2,597	2,094
Boston	3,417	1,305
Chicago	6,585	3,793
Dallas	4,128	3,131
Houston	3,019	2,365
Los Angeles	8,245	3,794
Miami	3,417	2,409
New York	14,326	7,464

Philadelphia	4,305	2,247
Phoenix	2,704	1,929
San Francisco	2,898	1,125
D.C.	3,576	2,159

3.2 Constructing Response Windows and Calculating ∇_{HDT}

In this session, we aim to capture the increase in home-dwelling time (∇_{HDT}) during the stay-at-home orders by constructing response windows. Given the discrepancy in the start/end date and the time duration of the stay-at-home orders in selected MSAs, we construct response windows specifically for each MSA. A response window is defined as a time interval that extends seven days before and after the duration when the stay-at-home order is effective. Such a fourteen-day extension to the original stay-at-home order aims to better capture the disparity in response from CBGs with different societal settings, as studies have found contrasting mobility patterns from different communities shortly prior to and following the orders (Gao et al. 2020; Huang et al. 2020a; Huang et al. 2020b; Weill et al. 2020). Appendix Figure B presents the summary of stay-at-home orders in the twelve selected MSAs (based on state-wide orders).

For a CBG, as above-mentioned, HDT_i denote its sampled mobile device accompanied residents' median home-dwelling time on day i . We define ∇_{HDT} as:

$$\nabla_{HDT} = \text{median}(HDT_m, HDT_{m+1} \dots HDT_n) - \text{median}(HDT_1, HDT_2 \dots HDT_{m-1}) \quad (1)$$

where *median* denotes the median operator, HDT_1 denotes the home-dwelling time on the first day of the time series (January 1, 2020), and records from HDT_m to HDT_n denote the home-dwelling time within the response window of that CBG. The calculated ∇_{HDT} in a certain CBG represents the amount of increased home-dwelling time, reflecting the impact of COVID-19 on outdoor activities as well as the compliance of the stay-at-home order.

3.3 Pearson Correlation and Random Forest Regression

To understand the contribution of demographic and socioeconomic variables to ∇_{HDT} in each MSA, we first perform a Pearson correlation to reveal the bivariate correlation between ∇_{HDT} and each individual demographic/socioeconomic variable. We test the Pearson's r at three significance levels: $\alpha = 0.05, 0.01, 0.001$. Numerous studies have suggested that variables describing demography and socioeconomic status tend to present

high multicollinearity (Wen et al. 2003; Leal et al. 2012; Gayer 2000), which violates the underlying assumption of independence in many regression approaches (e.g., multiple regression). Besides, the impact of those variables on ∇_{HDT} might not be linear. Given the above considerations, we chose the Random Forest Regressor because of its capability in handling non-linear parameters while preventing overfitting, tolerance to outliers, and scaling-free nature. Random Forest is a bagging-based algorithm that applies an ensemble learning technique by constructing a multitude of decision trees at training time (Liw and Wiener 2020). For each MSA, we divide its CBGs into a training set (70%) and a testing set (30%). The Random forest model takes the following summarized steps (with n_{tree} and m_{try} as two major hyperparameters):

- (1) A total of n_{tree} bootstrap samples, i.e., $S_1, S_2 \dots S_{n_{tree}}$, are drawn with replacement from the training set in that MSA. A bootstrap subset contains approximately one-third of the records in the training set. The elements not included in a bootstrap subset are referred to as out-of-bag (OOB) data.
- (2) The bootstrap samples are used to grow an unpruned regression tree: at each node, a total of m_{try} predictor variables are randomly selected, and the best split is chosen from among these variables. A prediction function is therefore formed for each bootstrap subset: $\hat{Y}_1 = \hat{f}(X, S_1), \hat{Y}_2 = \hat{f}(X, S_2), \dots, \widehat{Y_{n_{tree}}} = \hat{f}(X, S_{n_{tree}})$.
- (3) The OOB data are predicted by averaging the predictions from n_{tree} trees.

$$\hat{Y} = \frac{1}{n_{tree}} \sum_{k=1}^{n_{tree}} \hat{f}(X, S_k)$$
. The importance of each predictor is further measured by calculating the percent increase in Mean Square Error (MSE).

For each MSA, the hyperparameters (n_{tree} and m_{try}) of its Random Forest model are fine-tuned via the Grid Search approach (Bao and Liu 2006). The search space for n_{tree} is confined in [10,1000] with the value of 10 as the interval, while $m_{try} \in \{S, \frac{S}{2}, \frac{S}{3}, \sqrt{S}, \log_2(S)\}$. After fine-tuning, the Random Forest model with the best parameter setting for a certain MSA is applied to its testing set for evaluation. The goodness-of-fit (R^2) is reported for each Random Forest model to reflect how closely the predicted ∇_{HDT} matches the observed ∇_{HDT} . In each MSA, the R^2 of its Random Forest model is defined as:

$$R^2 = 1 - \frac{\sum_{i=1}^n (\nabla_{HDT}^i - \widehat{\nabla_{HDT}^i})^2}{\sum_{i=1}^n (\nabla_{HDT}^i - \overline{\nabla_{HDT}^i})^2} \quad (2)$$

where n denotes the number of CBGs in the testing set, $\widehat{\nabla_{HDT}^i}$ denotes the predicted value of ∇_{HDT}^i , and $\overline{\nabla_{HDT}^i}$ denotes the mean of all ∇_{HDT}^i within that MSA.

We also present the feature importance to shed light on each selected variable's relative importance when a MSA's optimized Random forest model makes the prediction. The ranking of variables based on the importance score suggests the different degrees of contribution in the Random Forest model. The partial dependence is further presented to reveal the dependence between the ∇_{HDT} and the most dominant variable, marginalizing over the values of all other variables, which allows us to gauge how a change in the most dominant variable affects the change in ∇_{HDT} .

5 Results

5.1 The distribution of ∇_{HDT}

To understand how different MSAs respond to the stay-at-home orders, we apply the kernel density estimation (analogous to a histogram) to reveal the distributing pattern of ∇_{HDT} (Figure 4). The shape of the distribution of ∇_{HDT} generally reflects the CBGs' demographic and societal characteristics within the MSA. In general, a dominant number of CBGs present a positive ∇_{HDT} , indicating a general trend of increased home-dwelling time under the stay-at-home orders. The distribution of ∇_{HDT} in twelve selected MSAs generally presents considerable normality and low skewness, except that Philadelphia MSA, San Francisco MSA, and Los Angeles MSA show a slight tendency towards bimodal distribution (Figure 4). Such a tendency presumably results from the differing strictness in mitigation measures due to their administrative-polycentric nature and heterogeneity. Despite that stay-at-home orders and social distancing guidelines have been issued in all MSAs, the effectiveness of these orders show notable discrepancies, evidenced by the varying median and mean values in ∇_{HDT} . As expected, New York MSA, the first-wave epicenter of COVID-19, shows the highest ∇_{HDT} . The mean ∇_{HDT} among all CBGs in New York MSA reaches 369.7 mins, suggesting that residents spend six hours more on average under the stay-at-home order. San Francisco MSA and Philadelphia MSA also present relatively high ∇_{HDT} (above 300 mins), indicating the

strong impact of stay-at-home orders on the out-of-home activities of their residents. In contrast, Phoenix MSA presents the lowest ∇_{HDT} with both mean and the median less than 200 mins. A similar weak response to the stay-at-home orders can also be found in Houston MSA and Chicago MSA. The revealed disparity in ∇_{HDT} at the MSA level presumably results from the heterogeneity among MSAs, such as the varying strictness in mitigation measures, varying political affiliations, and varying level of risk awareness.

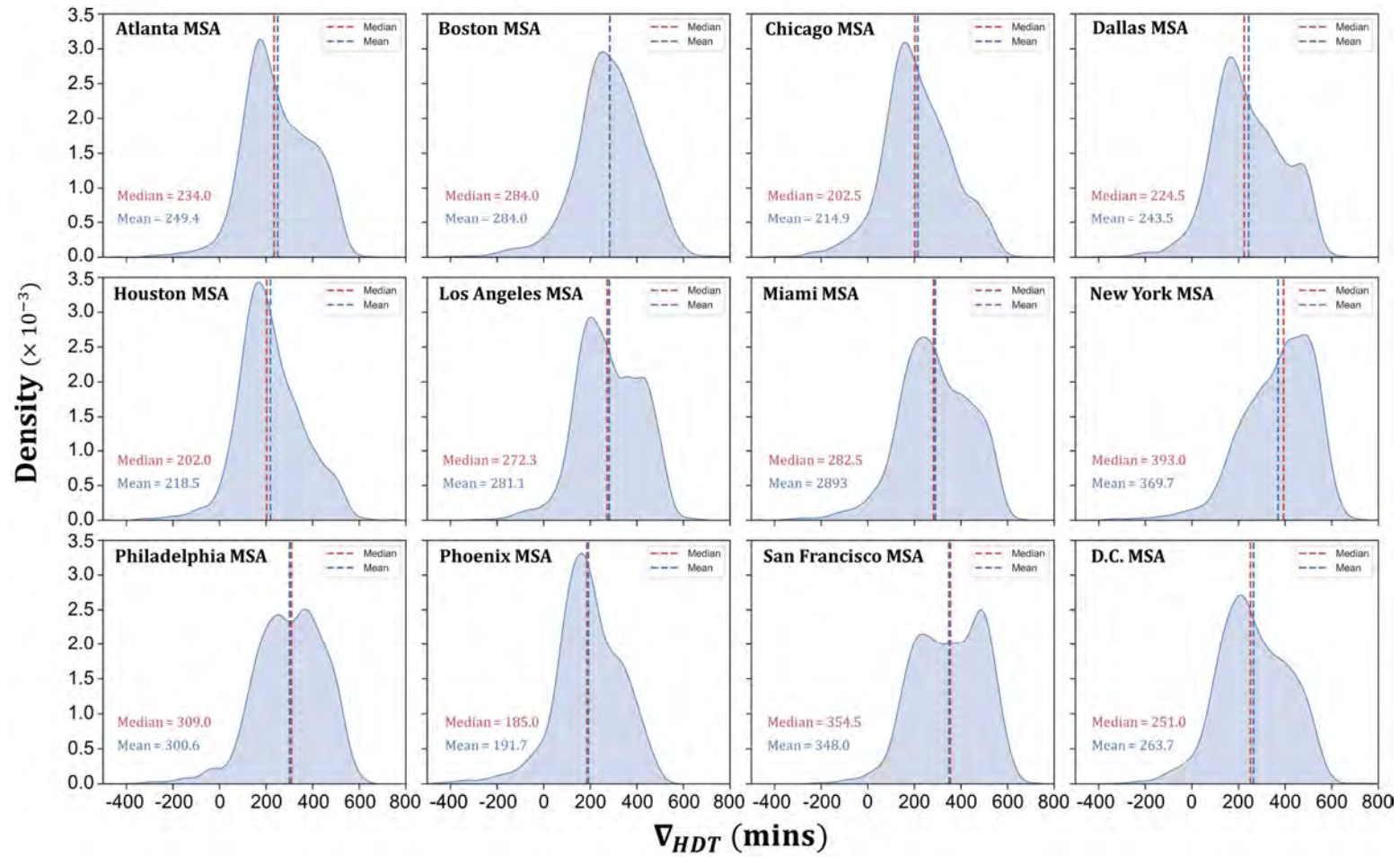


Figure 4. The distribution of ∇_{HDT} in twelve selected MSAs.

5.2 Pearson Correlation Between ∇_{HDT} and Demographic/Socioeconomic Variables

We first evaluate the bivariate correlation between ∇_{HDT} and each individual demographic/socioeconomic variable via Pearson correlation. Table 3 presents Pearson's r in all twelve MSAs, tested at three significance levels: $\alpha = 0.05, 0.01, 0.001$. The correlations between ∇_{HDT} and variables that describe economic status (*% low income, % high income, % unemployment, and median hhinc*) are significant at $\alpha = 0.001$ in all MSAs. Variables that include *% high income* and *median hhinc* show a strong positive correlation ($r > 0.5$) in most MSAs, suggesting that the group of people in CBGs with a higher percentage of wealthy residents and with a higher general income level tend to spend more time at home under the stay-at-home orders. This finding coincides with other studies in the U.S. at different scales, pointing out the luxury nature of social distancing guidelines (Huang et al. 2020a; Weill et al. 2020). Variables relating to educational level also present a strong and statistically significant correlation with ∇_{HDT} , with the percentage of low/high education in CBGs showing a contrasting direction in correlation. The group of people in CBGs with higher percent of master, professional, or doctoral degrees had a higher compliance level and stayed at home longer. The correlation between ∇_{HDT} and racial and ethnic variables are generally in agreement in the selected MSAs, but with several exceptions. For instance, in Miami MSA, the percentage of Hispanic shows a positive correlation with ∇_{HDT} , contradicting the negative correlations found in other MSAs. The percentage of Asian shows a statistically significant positive correlation in all MSAs, except Boston MSA. Car ownership generally shows a stronger correlation with ∇_{HDT} compared to other transportation-related variables. In most MSAs, the correlation between Gender (*% female*) and ∇_{HDT} is not significant. Even in MSAs that Gender presents significance (e.g., New York MSA and Los Angeles MSA), its strength is found rather weak.

Table 3. Pearson correlation coefficient (Pearson's r) between selected demographic/socioeconomic variables and ∇_{HDT} .

Variables	Top twelve MSAs with most population											
	Atlanta	Boston	Chicago	Dallas	Houston	Los Angeles	Miami	New York	Philadel-phia	Phoenix	San Francisco	D.C.
<i>median hhinc</i>	0.64***	0.43***	0.53***	0.66***	0.61***	0.55***	0.51***	0.45***	0.53***	0.56***	0.59***	0.58***
<i>% female</i>	-0.04	0.00	-0.01	0.01	0.07**	0.04**	0.05*	-0.06***	-0.04	0.02	0.07*	0.00
<i>% child</i>	-0.12***	-0.04	-0.05**	-0.13***	-0.10***	-0.14***	-0.08***	-0.11***	-0.13***	0.03	-0.09**	-0.11***
<i>% schooler</i>	0.16***	0.22***	0.15***	0.10***	0.04**	-0.02	0.15***	0.10***	0.11***	0.27***	0.11***	0.25***
<i>% elderly</i>	0.12***	0.04	0.04**	0.11***	0.10***	0.30***	0.01	0.11***	0.12***	-0.20***	0.22***	0.06**
<i>% white</i>	0.26***	0.14***	0.16***	0.09***	0.09***	0.22***	0.30***	0.29***	0.31***	0.10***	0.17***	0.15***
<i>% black</i>	-0.29***	-0.12***	-0.19***	-0.20***	-0.20***	-0.20***	-0.32***	-0.33***	-0.32***	-0.06**	-0.35***	-0.20***
<i>% asian</i>	0.27***	0.02	0.25***	0.35***	0.36***	0.20***	0.18***	0.19***	0.12***	0.23***	0.25***	0.37***
<i>% hispanic</i>	-0.22***	-0.17***	-0.21***	-0.44***	-0.34***	-0.49***	0.14***	-0.31***	-0.25***	-0.26***	-0.53***	-0.25***
<i>% low edu</i>	-0.57***	-0.33***	-0.46***	-0.59***	-0.53***	-0.51***	-0.44***	-0.39***	-0.45***	-0.44***	-0.53***	-0.53***
<i>% grad edu</i>	0.52***	0.33***	0.49***	0.54***	0.51***	0.49***	0.43***	0.38***	0.43***	0.41***	0.52***	0.51***
<i>% unemployment</i>	-0.19***	-0.07**	-0.20***	-0.16***	-0.16***	-0.19***	-0.24***	-0.20***	-0.22***	-0.21***	-0.21***	-0.20***
<i>% low income</i>	-0.37***	-0.23***	-0.26***	-0.41***	-0.37***	-0.34***	-0.31***	-0.32***	-0.33***	-0.36***	-0.33***	-0.28***
<i>% high income</i>	0.64***	0.42***	0.56***	0.64***	0.60***	0.55***	0.49***	0.45***	0.53***	0.53***	0.61***	0.59***
<i>% car commuter</i>	-0.11***	0.03	-0.12***	-0.17***	-0.01	0.15***	0.07***	0.15***	0.11***	0.03	0.05	0.08***
<i>% transit commuter</i>	-0.14***	-0.03	0.08***	-0.14***	-0.06**	-0.28***	-0.20***	-0.13***	-0.16***	-0.18***	-0.05	-0.16***
<i>% work from home</i>	0.41***	0.17***	0.28***	0.40***	0.24***	0.26***	0.20***	0.15***	0.27***	0.20***	0.23***	0.29***
<i>% short commuter</i>	-0.11***	-0.09**	-0.10***	-0.12***	-0.11***	0.04*	-0.08***	0.00	-0.02	-0.12***	-0.03	-0.13***
<i>% long commuter</i>	0.08***	0.14***	0.09***	0.05**	0.13***	0.03	0.17***	0.06***	0.06**	0.02	0.07*	0.03
<i>% 0car</i>	-0.28***	-0.20***	-0.19***	-0.28***	-0.30***	-0.30***	-0.31***	-0.30***	-0.29***	-0.28***	-0.25***	-0.27***
<i>% single parent</i>	-0.38***	-0.25***	-0.32***	-0.40***	-0.35***	-0.35***	-0.33***	-0.37***	-0.36***	-0.33***	-0.42***	-0.33***

*. Correlation significant at 0.05 level.

**. Correlation significant at 0.01 level.

***. Correlation significant at 0.001 level.

Pearson's $r > |0.5|$ is highlighted in bold.

5.3 Performance of the Optimized Random Forest Regressors

After the parameter fine-tuning process, the Random Forest model with the best parameter setting for each MSA is applied to the testing set for evaluation. Figure 5 presents the predicted ∇_{HDT} and observed ∇_{HDT} of CBGs in twelve selected MSAs with their goodness-of-fit (R^2). In general, the optimized Random Forest regressors well predict the ∇_{HDT} based on provided demographic/socioeconomic variables without notable systematic bias, as the regression line (red) is well aligned with the 1:1 reference line (black dashed) (Figure 5). It suggests that selected variables are potentially responsible for the ∇_{HDT} and are able to explain the variance in ∇_{HDT} via an ensemble tree-based regression design. However, the performance of the model varies considerably in different MSAs. Dallas MSA shows the highest $R^2 = 0.53$, followed by Atlanta MSA ($R^2 = 0.49$), D.C. MSA ($R^2 = 0.43$), and Houston MSA ($R^2 = 0.41$). The good performance of the optimized Random Forest model implies the prominent contribution of selected variables in predicting ∇_{HDT} especially in these MSAs. In comparison, Boston MSA, the only MSA that shows R^2 below 0.3, presents the lowest $R^2 = 0.21$. The low R^2 in Boston MSA partly results from its small sample size, as Boston MSA has the lowest number of available CBGs after preprocessing (Table 2). It can also be explained by the existence of many outlying CBGs with a negative ∇_{HDT} . The abnormal pattern in CBGs with decreased home-dwelling time under the stay-at-home order fails to be explained by the variables in the model, leading to inaccurate predictions.

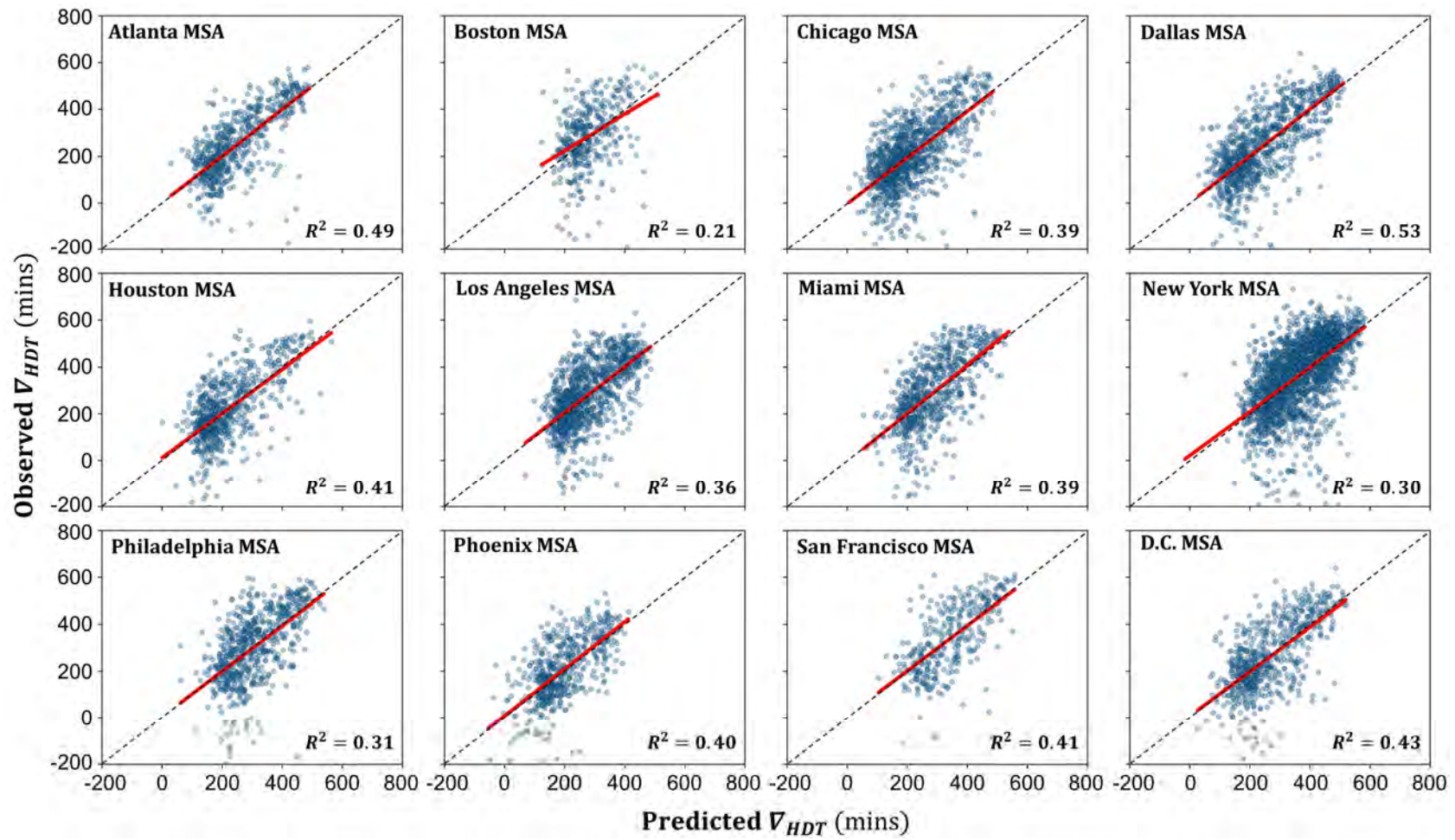


Figure 5. Predicted ∇_{HDT} and observed ∇_{HDT} of CBGs in twelve selected MSAs.

5.4 Feature Importance and Partial Dependence

The feature importance of variables is produced by the optimized Random Forest structure of each MSA. It is computed based on the rule of variance reduction that guides the selection of internal nodes within a tree structure (Altmann et al. 2010). For a Random Forest model, the impurity decrease from each variable can be averaged over all trees, and the variables are therefore ranked according to this measure. Appendix Figure C presents the ranked feature importance (in descending order) of selected demographic/socioeconomic variables in each MSA, showing their relative importance in each MSA when the model makes the prediction. Figure 6 presents the integrated feature importance summarizing the importance scores from all MSAs. Despite the fact that MSA's Random Forest Regressors are optimized independently, the distribution of their feature importance shows a similar pattern, especially for variables with a high importance score. In most MSAs, median household income (*median hhinc*) is the variable with the highest feature importance. For MSAs where median household income is not the highest, i.e., Chicago MSA, New York MSA, and Los Angeles MSA, the percentage of high income (*% high income*) is with the highest importance. The integrated feature importance for all MSAs also points out the dominant contribution of economic variables in predicting ∇_{HDT} (Figure 6). Coupled with the identified strong positive correlation between economic variables and ∇_{HDT} (Table 3), we conclude that stay-at-home orders are with a unique luxury nature that low-income groups, to some degree, can not afford. Educational variables contribute to the prediction of ∇_{HDT} with relatively high importance, as the percentage of low education (*% low edu*) and the percentage of graduate education (*% grad edu*) rank the third and the fifth, respectively, within the twelve MSAs (Figure 6). The percentage of schoolers (*% schooler*) also plays an important role, ranking the fourth in feature importance (Figure 6).

The partial dependence shows the marginal effect one variable has on the predicted outcome of a machine learning model (Friedman 2001), which facilitates our understanding of the causal relationship between the investigated variable and the prediction. Here, we present the partial dependence of median household income (*median hhinc*), the most dominant variable, to gauge how its changes affect the changes in ∇_{HDT} (Figure 7). A general pattern can be observed that ∇_{HDT} increases with the increase of *median hhinc*, which is also confirmed by their positive bivariate correlation presented in

Table 3. Despite the similarity in the general tendency, however, the partial dependence is rather complex, and the trend differs among MSAs. In Boston, ∇_{HDT} increases remarkably when *median hhinc* increases from \$100,000 to \$120,000. Similar jumps of ∇_{HDT} can be found in Dallas MSA and Atlanta MSA when *median hhinc* increases from \$80,000 to \$100,000, in D.C. MSA when *median hhinc* increases from \$110,000 to \$120,000, and in New York MSA when *median hhinc* increases from \$40,000 to \$50,000. Such non-linear partial dependence between ∇_{HDT} and *median hhinc* suggests the changing importance of income in varying income intervals, and the dynamics of the importance of *median hhinc* is place-dependent.

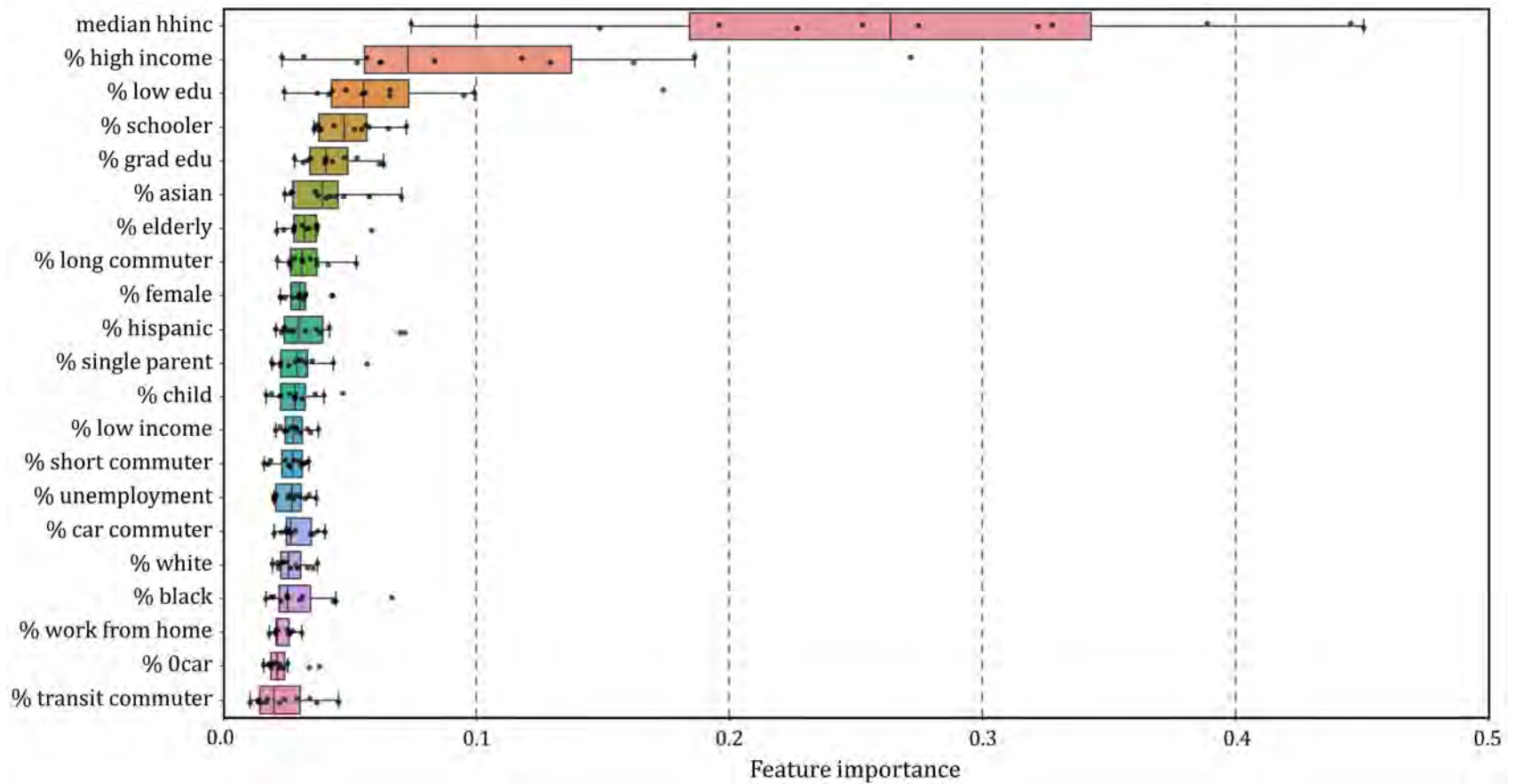


Figure 6. Integrated feature importance plot by combining importance scores in all selected MSAs. Variables are ranked in a descending order based on their median values.

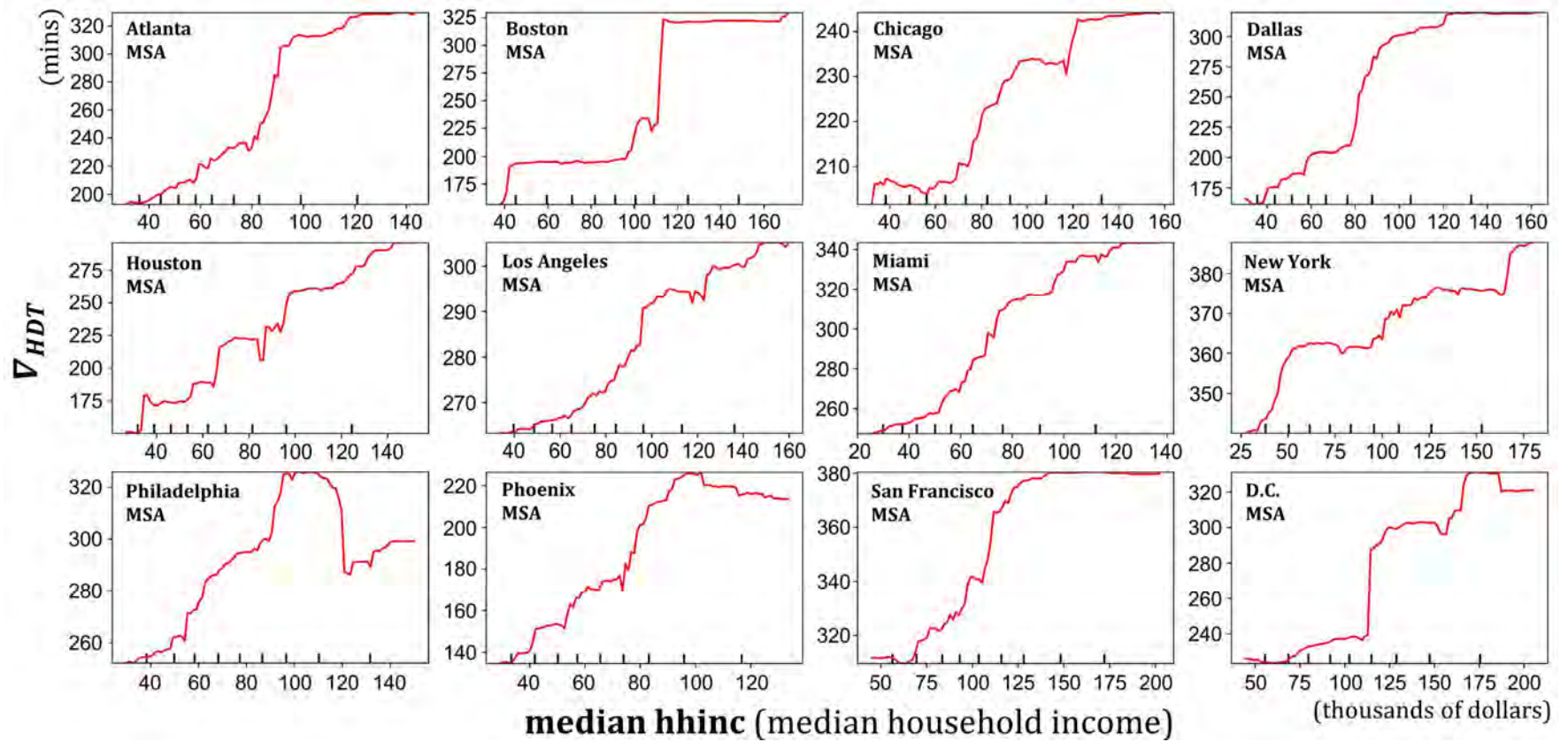


Figure 7. Partial dependence plot between median household income and V_{HDT} .

6 Discussion

6.1 What do we learn?

This study examines the stay-at-home compliance at the CBG level in twelve selected Metropolitan Statistical Areas (MSAs) via fine-grained home-dwelling records collected from millions of mobile devices. Despite the similarity in the general increasing trend of home-dwelling time under stay-at-home orders, each MSA presents its unique pattern, revealing the discrepancy in mitigation measures and the inconsistency in responses following these measures. Before we illustrate the role of variables and present reasonable explanations of their correlation with ∇_{HDT} and their general feature importance from those optimized Random Forest models, we need to acknowledge that demographic and socioeconomic variables are intrinsically intertwined and may not be viewed as completely independent variables.

We find statistically significant correlations between the increase in home-dwelling time (∇_{HDT}) and variables that describe economic status in all MSAs, revealing that the poor communities tend to show less compliance evidenced by their less dwelling time at home under the stay-at-home orders than the wealthy communities. The optimized Random Forest models also confirm this finding, as median household income and percentage of high income are the top two most important variables in predicting ∇_{HDT} , pointing out the unique luxury nature of stay-at-home orders in all MSAs with which lower-income groups may not afford to comply. The partial dependence between median household income and ∇_{HDT} suggests that the contribution of income to ∇_{HDT} is place-dependent, non-linear, and different given varying income intervals. It is reasonable to assume that the disparity in home-dwelling time between lower-income and upper-income groups leads to disparate exposures to the risk from the COVID-19. As lower-income communities already experience worse health outcomes and have a lower capacity to cope with economic and health shocks (Weill et al. 2020), their less compliance with stay-at-home orders might further exacerbate the situation.

The bivariate correlations between ∇_{HDT} and racial and ethnic variables are generally in agreement in selected MSAs. CBGs with a higher White percentage tend to present a higher ∇_{HDT} , while CBGs with a higher Black percentage tend to present a lower ∇_{HDT} . The percentage of Hispanic shows a negative correlation with ∇_{HDT} in all MSAs

except Miami MSA. The above evidence suggests that racial/ethnic minority populations spend less time at home during the stay-at-home orders, thus are generally more exposed to COVID-19 risk. Studies found that racial/ethnic minorities and poor people in urban settings live in more crowded conditions and comprise a higher percentage of workers in essential industries (Tai et al. 2020). Coupling with their disproportionate health burden of underlying comorbidities (e.g., diabetes, obesity, and coronary artery disease) (Cunningham et al. 2017; Tai et al. 2020) and lower access to healthcare (Godley et al. 2003; Waidmann and Rajan 2000), such exposure might contribute to disparities in COVID-19 outcomes that disfavor racial/ethnic minority populations. Despite the significant bivariate correlations between ∇_{HDT} and racial/ethnic variables, the feature importance scores suggest their trivial contribution to the prediction of ∇_{HDT} . This phenomenon can be explained by the calculation of the importance score in a Random Forest model, which prioritizes variables with a higher contribution by suppressing the importance of other highly correlated variables.

Variables relating to educational level also present a strong and statistically significant correlation with ∇_{HDT} , with the percentage of low/high education in CBGs showing a contrasting direction in correlation. They contribute to the prediction of ∇_{HDT} with relatively high importance, as the percentage of low education and the percentage of graduate education rank the third and the fifth, respectively. Generally, the higher rate of people with a low education degree, the less time they spend at home, and vice versa. On the one hand, occupations held by people with different education levels are more often different in terms of demands for physical proximity (Lekfuangfu et al. 2020), meaning that people with lower education levels have fewer economic opportunities, and the jobs they acquire do not have a work-from-home option. On the other hand, higher educated people report greater self-control and are more likely to have higher risk awareness (Ross and Wu 1995), which also indirectly makes higher educated people less likely to engage in out-of-home activities during the stay-at-home orders.

Interestingly, the percentage of school-age children (aged 5-17) presents high-level importance (ranking the fourth) in the Random Forest models of twelve selected MSAs, indicating its strong contribution to the prediction of ∇_{HDT} . In most MSA, the increase in home-dwelling time during the stay-at-home orders tend to be larger in CBGs with a higher share of schoolers. School closures are one of the most consistent non-pharmaceutical interventions regarding the pandemic in the United States – all 50 states

closed K-12 (kindergarten to 12th grade) schools over ten days in March (Donohue and Miler 2020). As a consequence, school-age children had to study at home all the time under the stay-at-home orders. Remote learning challenges and childcare duties forced parents to spend more time at home, which is a reasonable interpretation of our findings. Evidence shows that many parents spent a large amount of time with their child(ren) while schools were closed, and many of them were struggling with balancing their employment demands and childcare (Craig and Churchill 2020; Garbe et al. 2020; Wu and Xu 2020). It should also be noted that school closures could be a driver of increased unemployment during the pandemic (Kong and Prinz, 2020). This may be associated with the increased parenting time and workload at home caused by school closures. Commuting modes and travel time (*% car commuter, % transit commuter, % short commuter, and % long commuter*) are found trivial to the prediction of ∇_{HDT} , evidenced by their low feature importance in MSAs' optimized Random Forest models. Their correlations with ∇_{HDT} are weak and inconsistent (pointing to different directions with varying strength) among the twelve MSAs.

6.2 Limitations and Future Directions

It is important to acknowledge the limitations and provide guidelines for future studies. First, despite the widely recognized advantages of Random Forest models, several drawbacks need to be acknowledged and considered when the results of our study are interpreted. Hyperparameter settings play an important role in the performance of machine learning models, and tree-structure based Random Forest Regressor is no exception. To fine-tune the hyperparameters in each MSA's Random Forest Regressor, we use the Grid Search approach to find the optimal parameter settings from a designed parameter space. However, we might miss the best parameter settings as they may fall out of the designed parameter space. Studies are needed to further improve the optimization process by expanding the parameter searching space, despite the fact that a bigger search space can lead to more computational demand. We also need to acknowledge that the feature importance revealed by the Random Forest model tends to prioritize variables with a higher contribution by suppressing the importance of other highly correlated variables. Future studies can investigate the potential of other computationally costly importance measurements, such as permutation importance (Gregorutti et al. 2017) and drop-column importance (Parr et al. 2020). We use partial dependence to reveal potential causality existed between ∇_{HDT} and variable with the most

importance, i.e., median household income. However, partial dependence might hide the heterogeneous effects as it only shows the average marginal effects.

Second, the designed ∇_{HDT} represents the amount of increased home-dwelling time under stay-at-home orders, reflecting the general impact of COVID-19 on outdoor activities as well as the compliance of the stay-at-home order. It quantifies the increase in home-dwelling time during and before the stay-at-home orders, nonetheless neglecting the dynamics in the recovering phase (after reopening). Although the response window we construct is defined as a time interval that extends seven days before and after the duration when the stay-at-home order is effective, the long-term effects after reopening and the dynamics in time-series patterns are not thoroughly investigated in this study. Numerous studies have adopted trend-based time-series analytics to COVID-19 studies (Huang et al. 2020c; Chen et al. 2020). A possible future direction is to explore the potential of these approaches in better distinguishing the varying patterns in home-dwelling time.

Third, twenty-one variables are selected from five major categories in this study to explain ∇_{HDT} under stay-at-home orders, as numerous studies have proved their association with the participation of out-of-home activities. However, we need to acknowledge the potential contribution from the missing demographic/socioeconomic variables and other intangible factors that are hard to be quantified, such as risk awareness and belief in science. The inclusion of massive demographic/socioeconomic in regression inevitably introduces multicollinearity. One possible solution is to select uncorrelated and important components via Principal Component Analysis (PCA), a popular approach for dimensional reduction. Besides the demographic/socioeconomic perspective, future studies need to consider other underexplored aspects in order to better understanding the driving factors that lead to the disparity in compliance with stay-at-home orders.

Fourth, this study views each MSA as a spatial entity with a high degree of economic and social integration. However, we should acknowledge that mitigation measures might differ within a certain MSA, especially for urban and suburban regions. Such differences in measures may introduce a certain level of uncertainty into our study. In addition, we removed CBGs with insufficient device counts to ensure the credibility of the aggregated home-dwelling time. We observe that this preprocessing step excluded varying proportions of CBGs in different MSAs (see Table 2). Although the remaining CBGs are statistically enough for correlation analysis and training the Random Forest

models, the missing CBGs deserve further investigation to rule out the potential systematic bias in this data cleaning process.

Finally, the Random Forest model for each MSA is optimized without considering the inner spatial variation. Studies have revealed that built-up environment, socioeconomic activities, and demographic structure tend to vary substantially across densely populated urban fabrics (Nasri and Zhang 2012; Huang and Wong 2016), presumably leading to geographically-varying contribution of demographic/socioeconomic variables to the compliance with stay-at-home orders. Regression approaches that consider spatial nonstationarity, e.g., Geographically Weighted Regression (GWR) (Brunsdon et al. 1996), are great statistical tools to further explore the geographical variations within each MSA.

7 Conclusion

The COVID-19 pandemic has exposed, and to some degree, exacerbated the social inequity in the U.S. Taking advantage of the fine-grained mobile phone location tracking derived home-dwelling records at the U.S. Census Block Group (CBG) level and data-driven approaches, this study reveals the correlation between demographic/socioeconomic variables and home-dwelling time in twelve selected MSAs and further investigate the contribution of these variables to the disparity in home-dwelling time that reflects the compliance of stay-at-home orders using Random Forest models. The knowledge in this study deepens our understanding of social inequity issues exposed by the COVID-19 pandemic, greatly benefiting the decision-making of the Federal government and local authorities in choosing the appropriate response to the COVID-19 pandemic and future epidemics.

Despite the similarity in the general increasing trend of home-dwelling time under stay-at-home orders, we find that each MSA presents its unique pattern, revealing the discrepancy in mitigation measures and the inconsistency in responses following these measures. We find significant correlations in all MSAs between the increase in home-dwelling time (∇_{HDT}) and variables that describe economic status, revealing that the poor communities tend to show less compliance evidenced by their less time at home than the wealthy communities under the stay-at-home orders. Variables relating to educational level also present a strong and statistically significant correlation with ∇_{HDT} , with the percentage of low/high education in CBGs showing a contrasting direction in correlation.

The correlation between ∇_{HDT} and racial and ethnic variables are generally in agreement in the selected MSAs, but with several exceptions. The optimized Random Forest models we designed well predict the ∇_{HDT} based on provided demographic/socioeconomic variables without notable systematic bias. The median household income and percentage of high income are the top two most important variables in predicting ∇_{HDT} , pointing out the luxury nature of stay-at-home orders in all MSAs which lower-income groups can not afford. Educational variables contribute to the prediction of ∇_{HDT} with relatively high importance, as the percentage of low education and the percentage of graduate education rank the third and the fifth, respectively. The percentage of schoolers (age 5-17) also plays an important role, ranking the fourth in feature importance. The partial dependence between median household income and ∇_{HDT} suggests that the contribution of income to ∇_{HDT} is place-dependent, non-linear, and different given varying income intervals.

Our study reveals the geographical and social disparities in compliance with stay-at-home orders, potentially leading to disparate exposures to the COVID-19. Such disparate exposure to vulnerable populations can further compound by their other disadvantages, such as underlying comorbidities, poor access to and low utilization of high-quality health care, and limited access to COVID-19 testing centers, further causing negative health outcomes for the vulnerable populations. Thus, it is imperative to reduce immediate health effects and ensure equitable allocation of health care resources and the proper allocation of financial resources, such as subsidies, for more vulnerable populations. In the long term, we must confront systemic social inequity issues and call for a high-priority assessment of the long-term impact of COVID-19 on socially disadvantaged groups. It is never too late to act.

References

- Altmann, A., Toloși, L., Sander, O., and Lengauer, T. 2010. Permutation importance: a corrected feature importance measure. *Bioinformatics* 26(10): 1340-1347.
- Baek, C., McCrory, P.B., Messer, T., and Mui, P. 2020. Unemployment effects of stay-at-home orders: Evidence from high frequency claims data. Institute for Research on labor and employment working paper, pp.101-20.
- Bao, Y., and Liu, Z. 2006. A fast grid search method in support vector regression forecasting time series. In *International Conference on Intelligent Data*

Engineering and Automated Learning (pp. 504-511). Springer, Berlin, Heidelberg.

- Barnett-Howell, Z., and Mobarak, A.M. 2020. The Benefits and Costs of Social Distancing in Rich and Poor Countries. *arXiv preprint* arXiv:2004.04867.
- Barrios, J.M., and Hochberg, Y. 2020. Risk perception through the lens of politics in the time of the covid-19 pandemic. *National Bureau of Economic Research*. No. w27008.
- Bonaccorsi, G., Pierri, F., Cinelli, M., Flori, A., Galeazzi, A., Porcelli, F., Schmidt, A.L., Valensise, C.M., Scala, A., Quattrocioni, W., and Pammolli, F. 2020. Economic and social consequences of human mobility restrictions under COVID-19. *Proceedings of the National Academy of Sciences*, 117(27): 15530-15535.
- Briscese, G., Lacetera, N., Macis, M., and Tonin, M. 2020. Compliance with covid-19 social-distancing measures in italy: the role of expectations and duration. *National Bureau of Economic Research*. doi: 10.3386/w26916.
- Brodeur, A., Grigoryeva, I. and Kattan, L., 2020. Stay-At-Home Orders, Social Distancing and Trust. GLO Discussion Paper, No. 553, Global Labor Organization (GLO), Essen.
- Brunsdon, C., Fotheringham, A.S., and Charlton, M.E. 1996. Geographically weighted regression: a method for exploring spatial nonstationarity. *Geographical analysis* 28(4): 281-298.
- Chen, S.L.S., Yen, A.M.F., Lai, C.C., Hsu, C.Y., Chan, C.C., and Chen, T.H.H. 2020. An Index for Lifting Social Distancing During the COVID-19 Pandemic: Algorithm Recommendation for Lifting Social Distancing. *Journal of medical Internet research* 22(9): e22469.
- Chiou, L., and Tucker, C. 2020. Social distancing, internet access and inequality (No. w26982). *National Bureau of Economic Research*. doi: 10.3386/w26982.
- Craig, L., and Churchill, B. 2020. Dual-earner parent couples' work and care during COVID-19. *Gender, Work & Organization*. doi: 10.1111/gwao.12497.
- Cunningham, T.J., Croft, J.B., Liu, Y., Lu, H., Eke, P.I., and Giles, W.H., 2017. Vital signs: racial disparities in age-specific mortality among blacks or African Americans—United States, 1999–2015. *MMWR. Morbidity and mortality weekly report* 66(17): 444.

- Czeisler, M.É., Tynan, M.A., Howard, M.E., Honeycutt, S., Fulmer, E.B., Kidder, D.P., Robbins, R., Barger, L.K., Facer-Childs, E.R., Baldwin, G., and Rajaratnam, S.M. 2020. Public attitudes, behaviors, and beliefs related to COVID-19, stay-at-home orders, non-essential business closures, and public health guidance—United States, New York City, and Los Angeles, May 5–12, 2020. *Morbidity and Mortality Weekly Report*, 69(24): 751.
- Dasgupta, N., Funk, M.J., Lazard, A., White, B.E., and Marshall, S.W. 2020. Quantifying the social distancing privilege gap: a longitudinal study of smartphone movement. medRxiv. doi: 10.1101/2020.05.03.20084624.
- Donohue, J. M., and Miller, E. 2020. COVID-19 and school closures. *JAMA* 324(9): 845-847.
- Farber, S., and Páez, A. 2009. My car, my friends, and me: a preliminary analysis of automobility and social activity participation. *Journal of Transport Geography* 17(3): 216-225.
- Friedman, J.H. 2001. Greedy function approximation: a gradient boosting machine. *Annals of statistics* 29:1189-1232.
- Gao, S., Rao, J., Kang, Y., Liang, Y., Kruse, J., Dopfer, D., Sethi, A., Reyes, J., Yandell, B., and Patz, J. A. (2020). Association of mobile phone location data indications of travel and stay-at-home mandates with covid-19 infection rates in the us. *JAMA Network Open*, 3(9), e2020485-e2020485.
- Garbe, A., Ogurlu, U., Logan, N., and Cook, P. 2020. Parents' Experiences with Remote Education during COVID-19 School Closures. *American Journal of Qualitative Research* 4(3): 45-65.
- Gayer, T. 2000. Neighborhood demographics and the distribution of hazardous waste risks: An instrumental variables estimation. *Journal of regulatory economics* 17(2):131-155.
- Godley, P.A., Schenck, A.P., Amamoo, M.A., Schoenbach, V.J., Peacock, S., Manning, M., Symons, M., and Talcott, J.A. 2003. Racial differences in mortality among Medicare recipients after treatment for localized prostate cancer. *Journal of the National Cancer Institute* 95(22): 1702-1710.
- Gray, D.M., Anyane-Yeboa, A., Balzora, S., Issaka, R.B., and May, F.P. 2020. COVID-19 and the other pandemic: populations made vulnerable by systemic inequity. *Nature Reviews Gastroenterology & Hepatology* 17(9):520-522.

- Gregorutti, B., Michel, B., and Saint-Pierre, P. 2017. Correlation and variable importance in random forests. *Statistics and Computing* 27(3): 659-678.
- Huang, Q., and Wong, D.W. 2016. Activity patterns, socioeconomic status and urban spatial structure: what can social media data tell us?. *International Journal of Geographical Information Science* 30(9): 1873-1898.
- Huang, X., Li, Z., Jiang, Y., Li, X., and Porter, D. 2020c. Twitter reveals human mobility dynamics during the COVID-19 pandemic. *PloS one*, 15(11), e0241957.
- Huang, X., Li, Z., Jiang, Y., Ye, X., Deng, C., Zhang, J., and Li, X. 2020a. The characteristics of multi-source mobility datasets and how they reveal the luxury nature of social distancing in the US during the COVID-19 pandemic. *medRxiv*. doi: 10.1101/2020.07.31.20143016.
- Huang, X., Li, Z., Lu, J., Wang, S., Wei, H., and Chen, B. 2020b. Time-series clustering for home dwell time during COVID-19: what can we learn from it?. *ISPRS International Journal of Geo-Information*, 9(11), 675.
- Jones, B. 2020. Urban residents in states hit hard by COVID-19 most likely to see it as a threat to daily life. Accessed October 21. <https://www.pewresearch.org/fact-tank/2020/03/20/urban-residents-in-states-hit-hard-by-covid-19-most-likely-to-see-it-as-a-threat-to-daily-life/>.
- Kong, E., and Prinz, D. 2020. Disentangling policy effects using proxy data: Which shutdown policies affected unemployment during the COVID-19 pandemic?. *Journal of Public Economics*, 189: 104257.
- Kraemer, M.U., Yang, C.H., Gutierrez, B., Wu, C.H., Klein, B., Pigott, D.M., Du Plessis, L., Faria, N.R., Li, R., Hanage, W.P., and Brownstein, J.S. 2020. The effect of human mobility and control measures on the COVID-19 epidemic in China. *Science* 368(6490): 493-497.
- Kuppam, A.R., and Pendyala, R.M. 2001. A structural equations analysis of commuters' activity and travel patterns. *Transportation* 28(1): 33-54.
- Leal, C., Bean, K., Thomas, F., and Chaix, B. 2012. Multicollinearity in associations between multiple environmental features and body weight and abdominal fat: using matching techniques to assess whether the associations are separable. *American journal of epidemiology* 175(11): 1152-1162.

- Lekfuangfu, W.N., Piyapromdee, S., Porapakkarm, P., and Wasi, N. 2020. On Covid-19: New Implications of Job Task Requirements and Spouse's Occupational Sorting. SSRN 3583954. doi: 10.2139/ssrn.3583954.
- Liaw, A., and Wiener, M.. 2002. Classification and regression by randomForest. *R news* 2(3):18-22.
- Morency, C., Paez, A., Roorda, M.J., Mercado, R., and Farber, S. 2011. Distance traveled in three Canadian cities: Spatial analysis from the perspective of vulnerable population segments. *Journal of Transport Geography* 19(1): 39-50.
- Nasri, A., and Zhang, L. 2012. Impact of metropolitan-level built environment on travel behavior. *Transportation Research Record* 2323(1): 75-79.
- Oyedotun, T. D. T., and Moonsammy, S. 2020. Spatiotemporal Variation of COVID-19 and Its Spread in South America: A Rapid Assessment. *Annals of the American Association of Geographers*, doi: 10.1080/24694452.2020.1830024.
- Painter, M., and Qiu, T. 2020. Political beliefs affect compliance with covid-19 social distancing orders. SSRN. doi: 10.2139/ssrn.3569098.
- Parr, T., Wilson, J.D., and Hamrick, J. 2020. Nonparametric Feature Impact and Importance. *arXiv preprint arXiv:2006.04750*.
- Remuzzi, A., and Remuzzi, G. 2020. COVID-19 and Italy: what next?. *The Lancet* 395(10231): 1225-1228.
- Ross, C.E., and Wu, C.L. 1995. The links between education and health. *American sociological review* 60(5): 719-745.
- SafeGraph — Social Distancing Metrics. 2020. Accessed October 23.
<https://docs.safegraph.com/docs/social-distancing-metrics>.
- SafeGraph, What about bias in the SafeGraph dataset? (2019),
<https://www.safegraph.com/blog/what-about-bias-in-the-safegraph-dataset>, last accessed on November 8, 2020
- Shim, E., Tariq, A., Choi, W., Lee, Y., and Chowell, G. 2020. Transmission potential and severity of COVID-19 in South Korea. *International Journal of Infectious Diseases* 93: 339-344.
- Stoecklin, S.B., Rolland, P., Silue, Y., Mailles, A., Campese, C., Simondon, A., Mechain, M., Meurice, L., Nguyen, M., Bassi, C., and Yamani, E. 2020. First cases of coronavirus disease 2019 (COVID-19) in France: surveillance, investigations and control measures. *Eurosurveillance*, 25(6): p.2000094.

- Tai, D.B.G., Shah, A., Doubeni, C.A., Sia, I.G., and Wieland, M.L. 2020. The disproportionate impact of COVID-19 on racial and ethnic minorities in the United States. *Clinical Infectious Diseases*. doi: 10.1093/cid/ciaa815.
- U.S. Census Bureau — Metropolitan and Micropolitan Statistical Areas Population Totals and Components of Change: 2010-2019. 2020a. Accessed October 22. <https://www.census.gov/data/tables/time-series/demo/popest/2010s-total-metro-and-micro-statistical-areas.html>.
- U.S. Census Bureau — Metropolitan and Micropolitan. 2020b. Accessed October 23. <https://www.census.gov/programs-surveys/metro-micro/about.html>.
- Waidmann, T.A., and Rajan, S. 2000. Race and ethnic disparities in health care access and utilization: an examination of state variation. *Medical care research and review* 57: 55-84.
- Weill, J.A., Stigler, M., Deschenes, O., and Springborn, M.R. 2020. Social distancing responses to COVID-19 emergency declarations strongly differentiated by income. *Proceedings of the National Academy of Sciences*, 117(33): 19658-19660.
- Weill, J.A., Stigler, M., Deschenes, O., and Springborn, M.R. 2020. Social distancing responses to COVID-19 emergency declarations strongly differentiated by income. *Proceedings of the National Academy of Sciences* 117(33): 19658-19660.
- Wen, M., Browning, C.R. and Cagney, K.A., 2003. Poverty, affluence, and income inequality: neighborhood economic structure and its implications for health. *Social science & medicine* 57(5): 843-860.
- Wilder-Smith, A., and Freedman, D.O. 2020. Isolation, quarantine, social distancing and community containment: pivotal role for old-style public health measures in the novel coronavirus (2019-nCoV) outbreak. *Journal of travel medicine* 27(2): p.taaa020.
- World Health Organization (WHO). COVID-19 Weekly Epidemiological Update. World Health Organization. Accessed October 20, 2020. <https://www.who.int/docs/default-source/coronaviruse/situation-reports/20201020-weekly-epi-update-10.pdf>
- Wu, Q., and Xu, Y. 2020. Parenting stress and risk of child maltreatment during the COVID-19 pandemic: A family stress theory-informed perspective. *Developmental Child Welfare*. doi: 10.1177/2516103220967937.

Appendix

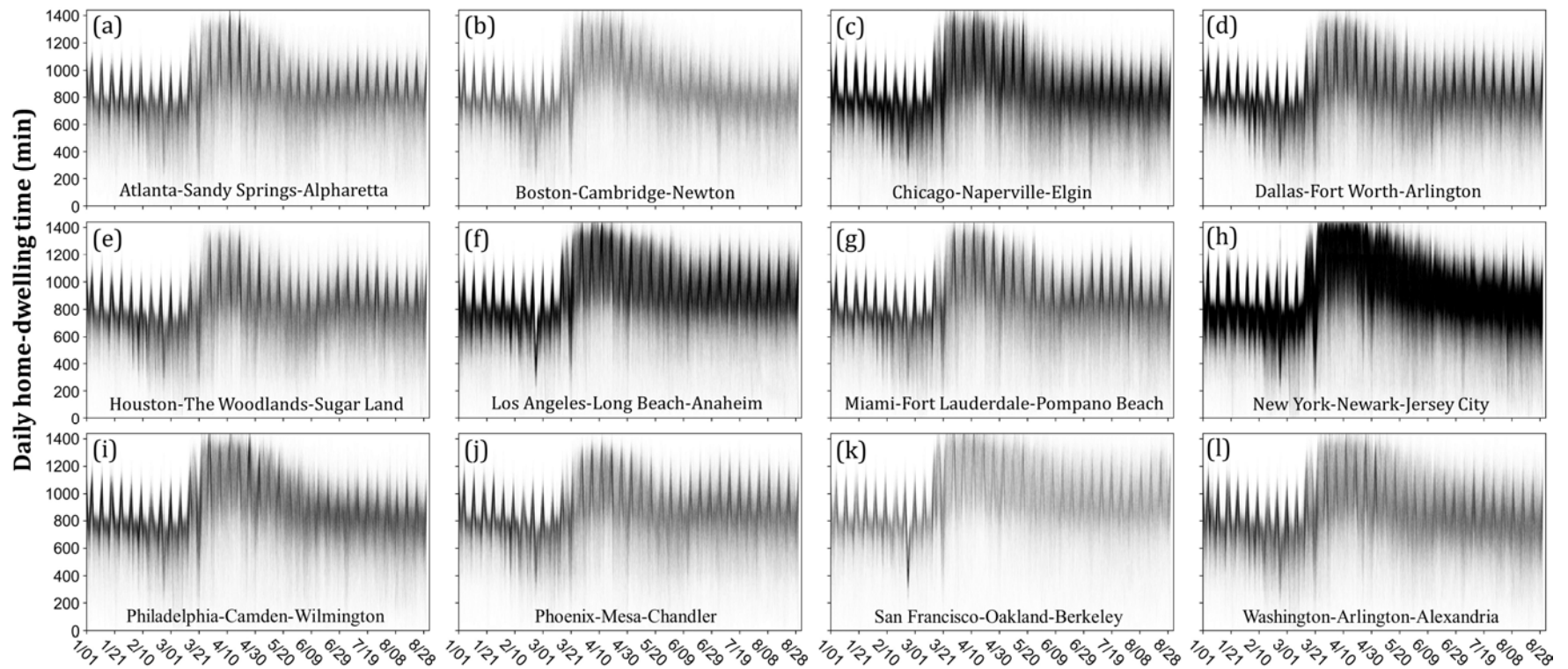


Figure A. Time-series density of daily home-dwelling time in twelve selected MSAs. The transparency for the time-series for each CBG is set as 0.01 ($\alpha = 0.01$).

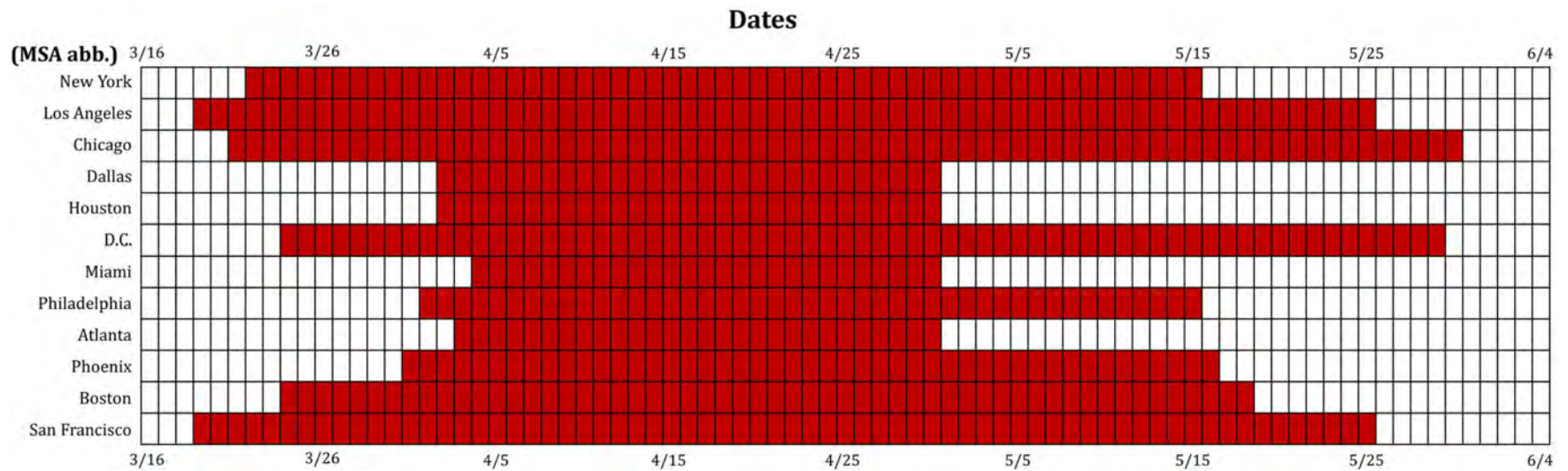


Figure B. The summarized issued dates of stay-at-home orders in the twelve selected MSAs (based on state-wide orders). The red blocks denote the effective dates. For a MSA that lies across multiple states, the state-wide order of the state that covers the most area of that MSA is used.

Source: *The New York Times* (<https://www.nytimes.com/interactive/2020/us/states-reopen-map-coronavirus.html>) and *Litter*

(<https://www.littler.com/publication-press/publication/stay-top-stay-home-list-statewide>)

